

# Reactivities of Amino Acid Derivatives Toward Hydrogen Abstraction by $\text{Cl}^\bullet$ and $\text{OH}^\bullet$

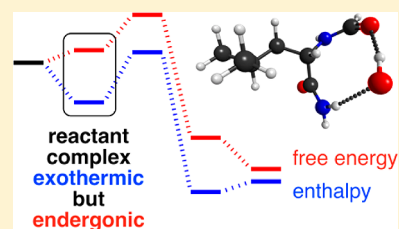
Bun Chan,<sup>\*,†,‡</sup> Robert J. O'Reilly,<sup>†,‡,||</sup> Christopher J. Easton,<sup>‡,§</sup> and Leo Radom<sup>\*,†,‡</sup>

<sup>†</sup>School of Chemistry, University of Sydney, Sydney, New South Wales 2006, Australia

<sup>‡</sup>ARC Centre of Excellence for Free Radical Chemistry and Biotechnology and <sup>§</sup>Research School of Chemistry, Australian National University, Canberra, Australian Capital Territory 0200, Australia

**S** Supporting Information

**ABSTRACT:** In recent computational studies of hydrogen-atom abstraction from amino acid derivatives, two distinct rationalizations have been put forward for the relative inertness of the  $\alpha$ -C–H. Of these, the proposal that the inertness is due to a “kinetic trap” associated with particularly stable complexes is shown to be unlikely because of unfavorable entropies. On the other hand, the proposed existence of deactivating polar effects at the  $\alpha$ -position in  $\text{Cl}^\bullet$  abstractions is likely also to be applicable to  $\text{OH}^\bullet$  abstractions, but to a lesser extent.



## INTRODUCTION

The carbon-centered radicals formed through hydrogen-atom abstraction from the  $\alpha$  (and to a lesser extent the  $\beta$ ) positions of the amino acid residues of proteins and peptides may undergo subsequent reactions, ultimately culminating in backbone cleavage.<sup>1</sup> It is therefore somewhat serendipitous that electrophilic free radicals (e.g.,  $\text{Cl}^\bullet$  and  $\text{OH}^\bullet$ ) appear to avoid abstraction from the  $\alpha$  and  $\beta$  positions, instead preferring to react (where possible),<sup>2,3</sup> with C–H moieties distal to these centers (see Figure 1),<sup>2,3</sup> producing radicals that are unlikely to

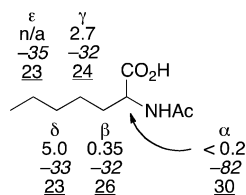


**Figure 1.** Experimental<sup>3</sup> relative rates for hydrogen abstraction by  $\text{Cl}^\bullet$  and corresponding calculated<sup>5</sup> free energies of reaction (in *italics*) and free energy barriers (underlined) ( $\text{kJ mol}^{-1}$ ).

lead to backbone cleavage. Indeed, it has even been suggested that a possible reason for nature selecting proteins as the building blocks of life is the innate resistance of this structural framework toward free-radical-induced degradation.<sup>3</sup> From the perspective of physical organic chemistry, this regioselectivity is peculiar, since abstraction from the  $\alpha$  carbon usually affords radical products that are overwhelmingly more stable compared with radicals formed along the aliphatic side chain, partially due to the existence of a captodative effect.<sup>4</sup>

In light of this remarkable regioselectivity, a number of theoretical studies have attempted to shed light on the origin of this contrathermodynamic effect in the context of abstractions by  $\text{Cl}^\bullet$  and  $\text{OH}^\bullet$ . Two differing explanations have been put

forward that are dependent on the nature of the abstracting radical.

For abstractions by  $\text{Cl}^\bullet$ , we have previously attributed the larger barrier associated with abstraction from the  $\alpha$  position (see Figure 1) to the existence of a deactivating polar effect.<sup>5</sup> In addition, we proposed that the early transition structure found in that case is particularly sensitive to such a polar effect, because the influence of the profound stability of the captodatively stabilized  $\alpha$ -radical product is reduced. In this regard, our findings are consistent with the longstanding experimentally held view that polar effects give rise to the regioselectivity of H abstraction by  $\text{Cl}^\bullet$ .<sup>2,6</sup>

On the other hand, for abstractions by  $\text{OH}^\bullet$  from *N*-formylleucinamide (1) (Figure 2), Scheiner and Kar concluded

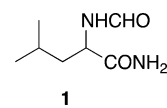


**Figure 2.** *N*-Formylleucinamide (1), a model for leucine residues in peptides.

that the larger barrier associated with abstraction from the  $\alpha$  position arises because of the formation of a particularly stable reactant complex at this position, which serves to act as a “kinetic trap”.<sup>7</sup> The formation of such complexes has also been invoked in explaining the kinetics of H abstraction by  $\text{OH}^\bullet$  from other amino acids, including glycine and alanine,<sup>8</sup> methionine,<sup>9</sup> asparagine,<sup>10</sup> isoleucine,<sup>11</sup> and serine.<sup>12</sup>

Although it is entirely possible that reactant complexes are important in determining the regioselectivity of H abstraction from amino acid derivatives by  $\text{OH}^\bullet$ , but not by  $\text{Cl}^\bullet$ , a unifying

Received: October 2, 2012

Published: October 12, 2012

explanation for the relative inertness in the two types of abstractions would be more appealing. In addition, the previous OH<sup>•</sup> investigations were based on considerations of enthalpies rather than free energies, thereby precluding consideration of the entropic penalty to be paid for the formation of such complexes. Indeed, in our previous investigation, we noted that, although binding of Cl<sup>•</sup> to *N*-acetylglycine is favorable on enthalpic grounds, such a complex is unfavorable on the free energy surface and therefore unlikely to be significant in determining the regioselectivity of H abstraction. In light of this finding, we felt it important to investigate whether similar conclusions might be reached in the case of the reactions involving OH<sup>•</sup>. To this end, we have re-evaluated the H abstraction from **1** by both OH<sup>•</sup> and Cl<sup>•</sup>, in the context of calculated free energies, and we now present our findings.

### COMPUTATIONAL DETAILS

We have used a theoretical approach that we have found previously to yield kinetics information of reasonable accuracy.<sup>5,13</sup>

Standard ab initio molecular orbital theory and DFT calculations<sup>14</sup> were carried out with Gaussian 09.<sup>15</sup> Gas-phase geometries of stationary points were obtained with the BHandH-LYP/6-31+G(d,p) procedure. We have briefly examined the conformational space of each relevant species, at the BHandH-LYP/6-31+G(d,p) level, in the same manner as in ref 5. Following each geometry optimization, harmonic frequency analysis was carried out to confirm the nature of the stationary point as an equilibrium structure or a transition structure. Improved single-point energies were evaluated using the B2K-PLYP procedure<sup>16</sup> in conjunction with the aug'-cc-pV(T+d)Z basis set, where aug' denotes the use of diffuse functions only on non-hydrogen atoms. The frozen-core approximation was used in all B2K-PLYP calculations. In order to account for the effect of spin-orbit coupling, literature values of 3.52 and 0.83 kJ mol<sup>-1</sup> were applied for the isolated Cl atom and OH radical, respectively.<sup>17</sup> We have assumed that the spin-orbit effect is quenched in the transition structure and in other regions of the reaction paths that we have examined.

To obtain the zero-point vibrational energies (ZPVEs) and thermal corrections for enthalpies ( $\Delta H_{298}$ ) and entropies ( $S_{298}$ ) at 298 K, we used BHandH-LYP/6-31+G(d,p) harmonic vibrational frequencies and appropriate literature scale factors.<sup>18</sup> A harmonic-oscillator rigid-rotor model is assumed in these calculations. For nonstationary points on reaction paths, the vibrations that correspond to the reaction coordinate are removed from the evaluation of ZPVEs and  $\Delta H_{298}$  and  $S_{298}$  values. For some nonstationary structures, harmonic vibrational analysis yields contentious low or imaginary frequencies. In those cases, the questionable frequencies are replaced by interpolated values obtained using formulas proposed by Truhlar and co-workers.<sup>19</sup>

The intrinsic reaction coordinate (IRC)<sup>20</sup> procedure was used to obtain reaction paths that connect transition structures with their adjacent minima. We employ the IRCmax method<sup>21</sup> to approximate a high-level reaction path, by carrying out high-level (B2K-PLYP) single-point energy calculations on a low-level (BHandH-LYP) IRC. Solvation corrections at each point on the reaction path were obtained at the M05-2X/6-31G(d) level using the SMD model, which has been shown to yield free energies of solvation for a wide range of neutral solutes with an overall uncertainty of ~3 kJ mol<sup>-1</sup>.<sup>22</sup> We find that this methodology produces standard free energies of solvation for OH<sup>•</sup> (-16.6 kJ mol<sup>-1</sup>), water (-28.6 kJ mol<sup>-1</sup>), and HCl (-5.4 kJ mol<sup>-1</sup>) that are in good agreement with the corresponding experimental values<sup>23</sup> of -16.3, -26.4, and -8.2 kJ mol<sup>-1</sup>. In order to best reflect experimental reaction conditions, we used the parameters for acetic acid for abstractions by Cl<sup>•</sup>, while for OH<sup>•</sup> abstractions the parameters for water were employed.

Rate constants ( $k$ ) at 298 K are obtained from the calculated free energy barriers ( $\Delta G^\ddagger$ ) using the standard Eyring expression:  $k = (k_B T/h) \exp(-\Delta G^\ddagger/RT)$ . These  $k$  values, together with the number of hydrogen atoms at each of the  $\alpha$ ,  $\beta$ ,  $\gamma$ , and  $\delta$  positions, were then used

to obtain our theoretical estimates of relative yields. All relative energies are given in kJ mol<sup>-1</sup>.

## RESULTS AND DISCUSSION

**Importance of Reactant Complexes.** We first consider whether reactant complexes play an important role in determining the kinetics of H abstraction from *N*-formylleucineamide (**1**) by Cl<sup>•</sup> and OH<sup>•</sup>. In addition to the complexes formed between **1** and either Cl<sup>•</sup> or OH<sup>•</sup> that are directly relevant to abstraction from the  $\alpha$ - $\delta$  positions, we have also considered complexes that may not directly lead to H abstraction but which nonetheless may act as kinetic traps for the abstractions. However, because the latter complexes are relevant to all the abstractions, they are unlikely to affect the relative propensities for abstraction at the various positions. Representative examples of the complexes are shown in Figure 3.

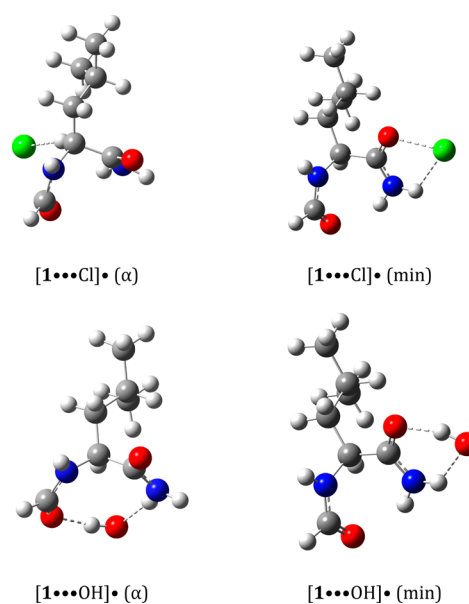


**Figure 3.** Geometries of complexes formed between **1** and Cl<sup>•</sup> or OH<sup>•</sup>.

Beginning with the interaction of Cl<sup>•</sup> with **1** (Table 1), we note that the complex of lowest energy (i.e., [1...Cl]<sup>•</sup>(min), Figure 3), which is not related to abstraction from any particular position, is predicted to be strongly bound on the enthalpic surface ( $\Delta H_C(\text{min}) = -33.4$  kJ mol<sup>-1</sup>) but only weakly bound in terms of free energy ( $\Delta G_{C,s}(\text{min}) = -6.5$  kJ mol<sup>-1</sup>). The complexes that are directly relevant to abstractions by Cl<sup>•</sup> from the  $\alpha$ - $\delta$  positions are all predicted to have positive free energies and thus would not form spontaneously; these are therefore unlikely to affect the regioselectivity of H abstraction by Cl<sup>•</sup>.

Turning our attention now to the complexes formed between **1** and OH<sup>•</sup>, we find that although the complex suggested by Scheiner and Kar to provide a kinetic trap hindering abstraction from the  $\alpha$ -position has a favorable enthalpic complexation energy ( $\Delta H_C(\alpha) = -35.0$  kJ mol<sup>-1</sup>), the inclusion of entropic contributions and solvation effects renders the binding unfavorable on the free energy surface ( $\Delta G_{C,s}(\alpha) = +21.7$  kJ mol<sup>-1</sup>). Regarding the large and positive  $\Delta \Delta G_{C,s}$  for both the minimum energy OH complex and the complex associated with  $\alpha$  abstraction, we note that the proton of the OH<sup>•</sup> moiety in

**Table 1. Solution-Phase Free Energies of Complexation ( $\Delta G_{C,s}$ ) between  $Cl^\bullet$  and  $OH^\bullet$  with *N*-Formylleucinamide (1) and Components Leading to These Values (298 K, kJ mol<sup>-1</sup>)<sup>a</sup>**

	$\Delta E_C$	$\Delta\Delta H_C$	$\Delta H_C$	$-T\Delta S_C$	$\Delta G_C$	$\Delta\Delta G_{C,s}$	$\Delta G_{C,s}$
<b><math>Cl^\bullet</math><sup>b</sup></b>							
$\alpha$	-1.3	1.4	0.1	22.3	22.3	0.1	22.5
$\beta$	-6.1	0.8	-5.3	21.5	16.2	5.6	21.8
$\gamma$	-11.1	1.7	-9.4	25.9	16.5	-4.8	11.7
$\delta$	-2.9	1.1	-1.8	14.5	14.5	0.7	13.3
min <sup>d</sup>	-35.3	1.9	-33.4	29.3	-4.1	-2.4	-6.5
<b><math>OH^\bullet</math><sup>c</sup></b>							
$\alpha$	-41.4	6.4	-35.0	35.7	0.7	20.9	21.7
$\beta$	-4.8	-0.8	-5.5	34.5	29.0	3.3	32.3
$\gamma$	5.1	1.9	6.9	25.4	32.3	1.5	33.7
$\delta$	-4.6	4.2	-0.3	19.3	19.0	1.9	20.9
min <sup>d</sup>	-37.9	6.2	-31.7	35.1	3.4	16.7	20.1

<sup>a</sup> $\Delta E_C$  = vibrationless gas-phase complexation energy (B2K-PLYP/ aug'-cc-pV(T+d)Z//BHandH-LYP/6-31+G(d,p)).  $\Delta\Delta H_C$  = correction for enthalpy at 298 K (inclusive of ZPVE).  $\Delta H_C$  = complexation enthalpy at 298 K ( $\Delta E_C + \Delta\Delta H_C$ ).  $-T\Delta S_C$  = entropic contribution.  $\Delta G_C$  = gas-phase free energy of complexation ( $\Delta H_C - T\Delta S_C$ ).  $\Delta\Delta G_{C,s}$  = solvation contribution.  $\Delta G_{C,s}$  = solution-phase free energy of complexation ( $\Delta G_C + \Delta\Delta G_{C,s}$ ). <sup>b</sup>Acetic acid solvent for  $\Delta\Delta G_{C,s}$ . <sup>c</sup>Water solvent for  $\Delta\Delta G_{C,s}$ . <sup>d</sup>Minimum energy complex that is not specific to abstraction from any of the positions (see Figure 3).

these complexes is involved in hydrogen bonding with **1** (Figure 3). Thus, we can expect this proton to be solvated less strongly than in an isolated  $OH^\bullet$ . As a result of all of the above effects, the formation of the  $\alpha$  complex is not spontaneous and is therefore unlikely to be important in determining the kinetics of H abstraction.

This finding contrasts with the conclusions reached previously based on the enthalpic surface,<sup>7</sup> which did not take into account the unfavorable entropic penalty (on the free energy surface) associated with the interaction of  $OH^\bullet$  with **1**. It therefore seems that the relatively inert nature of the  $\alpha$ -C-H in amino acid derivatives toward abstraction by  $OH^\bullet$  must have an alternative explanation, and we now proceed to explore this further.

**Barriers for Abstraction from Neutral *N*-Formylleucinamide.** We have computed both the gas-phase (Table 2) and solution-phase (Table 3) reaction free energies and barriers for the abstraction by  $Cl^\bullet$  and  $OH^\bullet$  from the various positions of **1** (i.e.,  $\alpha$ - $\delta$ ). Furthermore, in order to assist in elucidating the effects that give rise to the observed regioselectivity, we also provide the individual components that together result in the final free energy barriers. In the gas phase (Table 2), we find that the free energies of reaction ( $\Delta G_g$ ) become increasingly negative in the order  $\delta \rightarrow \beta \rightarrow \gamma \rightarrow \alpha$ , consistent with the expected relative stabilities of the carbon-centered radicals being formed: i.e., abstractions from  $CH_3 < CH_2 < CH$  leading to primary, secondary, and tertiary radicals, respectively. Formation of the  $\alpha$ -carbon-centered radical, which is subject to captodative stabilizing effects, has the greatest thermodynamic driving force ( $-61.9$  and  $-120.7$  kJ mol<sup>-1</sup> for abstractions by  $Cl^\bullet$  and  $OH^\bullet$ , respectively).

If we compare the barriers calculated at the two tertiary positions for H abstractions by both  $Cl^\bullet$  and  $OH^\bullet$ , we find that the barriers for abstraction from the  $\alpha$  position are larger than those for the  $\gamma$  position. This ordering is in contrast to thermodynamics but, even in the absence of solvation effects,

**Table 2. Gas-Phase Reaction Free Energies ( $\Delta G_g$ ) for Hydrogen Abstraction by  $Cl^\bullet$  and  $OH^\bullet$  from the  $\alpha$ ,  $\beta$ ,  $\gamma$ , and  $\delta$  Positions of **1**, along with Corresponding Free Energy Barriers ( $\Delta G_g^\ddagger$ ) and Their Components (298 K, kJ mol<sup>-1</sup>)<sup>a</sup>**

	$\Delta G_g$	$\Delta E_g^\ddagger$	$\Delta\Delta H_g^\ddagger$	$\Delta H_g^\ddagger$	$-T\Delta S_g^\ddagger$	$\Delta G_g^\ddagger$
<b><math>Cl^\bullet</math></b>						
$\alpha$	-61.9	8.5	-6.1	2.5	31.3	33.8
$\beta$	-21.1	-1.3	-9.9	-11.2	37.2	26.0
$\gamma$	-40.5	-6.5	-0.8	-7.3	34.0	26.7
$\delta$	-17.3	2.3	-5.0	-2.8	30.2	27.5
<b><math>OH^\bullet</math></b>						
$\alpha$	-120.7	-2.6	0.6	-1.9	41.9	40.0
$\beta$	-80.0	-12.8	1.6	-11.2	41.7	30.5
$\gamma$	-99.4	-3.8	-0.2	-4.0	39.8	35.7
$\delta$	-76.2	1.3	-0.3	1.0	40.3	41.3

<sup>a</sup> $\Delta G_g$  = gas-phase free energy of reaction (B2K-PLYP/ aug'-cc-pV(T+d)Z//BHandH-LYP/6-31+G(d,p)).  $\Delta E_g^\ddagger$  = vibrationless energy contribution to the gas-phase variational free energy barrier.  $\Delta\Delta H_g^\ddagger$  = corrections for 298 K enthalpy barrier (incorporating ZPVE).  $\Delta H_g^\ddagger$  = 298 K enthalpy barrier ( $\Delta E_g^\ddagger + \Delta\Delta H_g^\ddagger$ ).  $-T\Delta S_g^\ddagger$  = entropic contribution.  $\Delta G_g^\ddagger$  = gas-phase variational free energy barrier ( $\Delta H_g^\ddagger - T\Delta S_g^\ddagger$ ).

**Table 3. Solution-Phase Free Energy Barriers ( $\Delta G_s^\ddagger$ ) for Hydrogen Abstraction from the  $\alpha$ ,  $\beta$ ,  $\gamma$ , and  $\delta$  Positions of **1** by  $Cl^\bullet$  and  $OH^\bullet$ , and Their Components, and Solution-Phase  $\Delta G_s^\ddagger$  Values for Protonated **1** (298 K, kJ mol<sup>-1</sup>)<sup>a</sup>**

	$\Delta E^\ddagger$	$\Delta\Delta H^\ddagger$	$-T\Delta S^\ddagger$	$\Delta G^\ddagger$	$\Delta\Delta G_s^\ddagger$	$\Delta G_s^\ddagger$	$\Delta G_s^\ddagger(H^+)$
<b><math>Cl^\bullet</math><sup>b</sup></b>							
$\alpha$	8.6	-5.4	30.2	33.5	-3.6	29.9	41.0
$\beta$	-2.7	-6.1	34.8	26.0	4.6	30.7	33.8
$\gamma$	-6.5	-0.8	34.0	26.7	-2.0	24.8	22.8
$\delta$	0.2	-3.3	29.9	26.8	-0.1	26.6	26.9
<b><math>OH^\bullet</math><sup>c</sup></b>							
$\alpha$	-2.6	0.6	41.9	40.0	14.2	54.2	56.5
$\beta$	-12.8	1.6	41.7	30.5	26.5	57.0	64.1
$\gamma$	-6.9	1.2	39.5	33.8	11.0	44.8	50.3
$\delta$	1.3	-0.3	40.3	41.3	12.9	54.2	58.4

<sup>a</sup> $\Delta E^\ddagger$  = vibrationless energy contribution to the solution-phase variational free energy barrier (B2K-PLYP/ aug'-cc-pV(T+d)Z// BHandH-LYP/6-31+G(d,p)).  $\Delta\Delta H^\ddagger$  = corrections for 298 K enthalpy barrier (incorporating ZPVE).  $-T\Delta S^\ddagger$  = entropic contribution.  $\Delta G^\ddagger$  = gas-phase free energy contribution to the solution-phase free energy barrier ( $\Delta E^\ddagger + \Delta\Delta H^\ddagger - T\Delta S^\ddagger$ ).  $\Delta\Delta G_s^\ddagger$  = solvation contribution.  $\Delta G_s^\ddagger$  = solution-phase variational free energy barrier ( $\Delta G^\ddagger + \Delta\Delta G_s^\ddagger$ ). <sup>b</sup>Acetic acid solvent for  $\Delta\Delta G_s^\ddagger$ . <sup>c</sup>Water solvent for  $\Delta\Delta G_s^\ddagger$ .

already partially reflects experimental results in related systems.<sup>3</sup> We find that the transition structures for  $Cl^\bullet$  abstraction are "early", with  $Cl\cdots H$  distances  $>1.9$  Å. On the other hand, the transition structures for abstraction by  $OH^\bullet$  are not particularly early ( $HO\cdots H \approx 1.45$  Å for abstractions from the  $\alpha$ ,  $\beta$ , and  $\delta$  positions and 1.54 Å for  $\gamma$ -abstraction). Thus, one might expect reaction thermodynamics to play a smaller role in the  $Cl^\bullet$  abstraction than in the  $OH^\bullet$  abstraction. As we shall see, for the abstraction by  $Cl^\bullet$ , the contrathermodynamic behavior is consistent with a polar deactivating effect, where the  $\sigma$ -electron-withdrawing NHCHO and CONH<sub>2</sub> groups at the  $\alpha$  carbon disfavor hydrogen abstraction by the electrophilic  $Cl^\bullet$  radical. However, such a polar effect would appear to be less dominant in the  $OH^\bullet$  abstraction, due to the presence of relatively strong secondary interactions.



We now turn our attention to considering the effect of solvation on the H abstraction barriers (Table 3). First of all, we note that the locations of the solution-phase variational TSs along the reaction paths are in some cases identical with, and in other cases slightly different from, the gas-phase variational structures. This is reflected in the small differences in some cases in the gas-phase (Table 2) and solution-phase (Table 3)  $\Delta E^\ddagger$  and  $\Delta G_s^\ddagger$  values. We also note that the solvation contributions ( $\Delta\Delta G_s^\ddagger$ ) at the  $\alpha$ ,  $\gamma$ , and  $\delta$  positions are relatively close to one another, but the  $\Delta\Delta G_s^\ddagger$  values for  $\beta$  abstractions are somewhat more positive, for both  $\text{Cl}^\bullet$  and  $\text{OH}^\bullet$  abstractions. In comparing the barriers associated with abstraction by  $\text{Cl}^\bullet$  and  $\text{OH}^\bullet$  from the  $\alpha$  and  $\gamma$  positions, we see that abstractions from the former position are associated with barriers that are 5.1 and 9.4  $\text{kJ mol}^{-1}$  higher, respectively, than from the latter position.

**Effect of Protonation.** The experimental studies were performed under acidic conditions, and hence the amino acid derivatives might be subject to various degrees of protonation, but our solvation corrections, obtained using a continuum model, do not explicitly account for such effects. Partial protonation of the carbonyl moieties, associated for example with hydrogen bonding,<sup>24</sup> might be expected to accentuate the extent of deactivation at the  $\alpha$  position. Indeed, we previously found that full protonation of the amino group of norleucine results in an especially large deactivation at the  $\alpha$  and adjacent positions for the abstraction by  $\text{Cl}^\bullet$ .<sup>5</sup> Partial protonation of an amido carbonyl is likely to have a less marked effect, but it might nonetheless further disfavor abstraction from the  $\alpha$  position in comparison with the unprotonated substrate.

To this end, we have calculated the corresponding barriers for protonated **1** (Table 3,  $\Delta G_s^\ddagger(\text{H}^+-\mathbf{1})$ ). The result is that, for the abstraction by  $\text{Cl}^\bullet$ , there is a clear deactivating effect at the  $\alpha$  and (to a lesser extent) the  $\beta$  positions. We have further utilized the calculated solution-phase barriers for both **1** and  $\text{H}^+-\mathbf{1}$  to estimate approximate relative yields of the chlorinated products at the various positions. For **1**, such estimation leads to 3, 4, 24, and 68% for the  $\alpha$ ,  $\beta$ ,  $\gamma$  and  $\delta$  products, respectively. For  $\text{H}^+-\mathbf{1}$ , the corresponding values are 0 ( $\alpha$ ), 1 ( $\beta$ ), 46 ( $\gamma$ ), and 53% ( $\delta$ ). These compare reasonably well with the experimental relative yields<sup>3</sup> for chlorine abstraction from the closely related *N*-acetylleucine, for which the values for  $\alpha$ ,  $\beta$ ,  $\gamma$ , and  $\delta$  are 0, 0, 49, and 51%, respectively. For abstraction from protonated **1** by  $\text{OH}^\bullet$ , we find that the general trend for the barriers for  $\text{H}^+-\mathbf{1}$  is not very different from that for neutral **1**. This is perhaps not unexpected, as the polar deactivating effect of  $\text{OH}^\bullet$  is found experimentally to be somewhat less than that of  $\text{Cl}^\bullet$ .<sup>3</sup> Our calculated barriers for **1** correspond to approximate relative yields of 2 ( $\alpha$ ), 1 ( $\beta$ ), 85 ( $\gamma$ ), and 12 ( $\delta$ ) %, and for  $\text{H}^+-\mathbf{1}$  they are 6 ( $\alpha$ ), 1 ( $\beta$ ), 75 ( $\gamma$ ), and 18% ( $\delta$ ).

#### Structural and Intermolecular Effects in the Barriers.

To further elucidate the source of the observed variations in the abstraction barriers, we have divided each vibrationless barrier ( $\Delta E^\ddagger$ ) into a structural-distortion component ( $\Delta E_{\text{dist}}$ ) and a fragment-interaction component ( $\Delta E_{\text{int}}$ ) (Table 4).<sup>25</sup> The  $\Delta E_{\text{dist}}$  values indicate the energies required to distort the fully optimized reactant geometries to those in the transition structures, and  $\Delta E_{\text{int}}$  represents the energy change for bringing together the distorted fragments from infinite separation to form the transition structure. To allow for a more thorough analysis, we have also included other constituents of the solution-phase free energy barriers for both neutral and protonated **1**.

**Table 4. Structural-Distortion ( $\Delta E_{\text{dist}}$ ) and Fragment-Interaction ( $\Delta E_{\text{int}}$ ) Components of the Vibrationless Barriers for the Abstraction Reactions of **1** and  $\text{H}^+-\mathbf{1}$  by  $\text{Cl}^\bullet$  and  $\text{OH}^\bullet$ , and Other Constituents of the Solution-Phase Free Energy Barriers ( $\text{kJ mol}^{-1}$ )**

	$\Delta E_{\text{dist}}$	$\Delta E_{\text{int}}$	$\Delta\text{ZPVE}^\ddagger$	$\Delta\Delta H_{298-0}^\ddagger$	$-T\Delta S^\ddagger$	$\Delta\Delta G_s^\ddagger$	$\Delta G_s^\ddagger$
<b>1, Cl<sup>•</sup><sup>b</sup></b>							
$\alpha$	16.7	-8.1	-4.1	-1.3	30.2	-3.6	29.9
$\beta$	5.5	-8.2	-3.8	-2.3	34.8	4.6	30.7
$\gamma$	10.6	-17.1	1.3	-2.1	34.0	-2.0	24.8
$\delta$	2.0	-1.9	-1.5	-1.9	29.9	-0.1	26.6
<b>H<sup>+</sup>-1, Cl<sup>•</sup><sup>b</sup></b>							
$\alpha$	12.6	-1.4	-3.7	-1.5	34.3	0.6	41.0
$\beta$	6.7	0.5	-3.5	-2.0	32.9	-0.8	33.8
$\gamma$	2.8	-12.6	-2.2	-2.0	32.6	4.3	22.8
$\delta$	1.5	-2.1	-1.4	-2.0	31.5	-0.6	26.9
<b>1, OH<sup>•</sup><sup>c</sup></b>							
$\alpha$	17.1	-19.7	4.9	-4.3	41.9	14.2	54.2
$\beta$	4.8	-17.5	6.3	-4.7	41.7	26.5	57.0
$\gamma$	6.6	-13.4	5.4	-4.2	39.5	11.0	44.8
$\delta$	5.1	-3.8	3.8	-4.1	40.3	12.9	54.2
<b>H<sup>+</sup>-1, OH<sup>•</sup><sup>c</sup></b>							
$\alpha$	12.6	-13.3	3.7	-3.3	40.0	16.7	56.5
$\beta$	8.1	-1.6	2.1	-3.3	38.4	20.5	64.1
$\gamma$	5.3	-20.0	3.2	-2.9	38.5	26.2	50.3
$\delta$	5.9	3.3	0.8	-2.5	36.2	14.6	58.4

<sup>a</sup> $\Delta\text{ZPVE}^\ddagger$  = zero-point vibrational energy contribution to barrier.  $\Delta\Delta H_{298-0}^\ddagger$  = corrections for 298 K enthalpy barrier (excluding  $\Delta\text{ZPVE}^\ddagger$ ).  $-T\Delta S^\ddagger$  = entropic contribution.  $\Delta\Delta G_s^\ddagger$  = solvation contribution.  $\Delta G_s^\ddagger$  = solution-phase free energy barrier. <sup>b</sup>Solvent acetic acid for  $\Delta\Delta G_s^\ddagger$ . <sup>c</sup>Solvent water for  $\Delta\Delta G_s^\ddagger$ .

For the abstraction by  $\text{Cl}^\bullet$ , it is apparent that, for both **1** and  $\text{H}^+-\mathbf{1}$ ,  $\Delta E_{\text{dist}}$  and  $\Delta E_{\text{int}}$  represent the largest variations among the various factors. For the abstraction by  $\text{OH}^\bullet$ , there are also substantial variations in  $\Delta\Delta G_s^\ddagger$ . Abstraction from the most remote  $\delta$  position gives  $\Delta E_{\text{dist}}$  and  $\Delta E_{\text{int}}$  values that are both very small in magnitude. Thus, the magnitude of the overall free energy barrier at the  $\delta$  position is mainly governed by entropy and solvation. The  $\alpha$  abstractions have notably more positive  $\Delta E_{\text{dist}}$  values than the corresponding  $\beta$ ,  $\gamma$ , and  $\delta$  values. This can be attributed to the interruption of the intramolecular hydrogen bonding between the two  $\alpha$  substituents in the  $\alpha$  transition structures (Figure 4).

We now turn our attention to  $\Delta E_{\text{int}}$ . It can be seen that, with the exception of  $\text{OH}^\bullet$  abstraction from neutral **1**,  $\Delta E_{\text{int}}$  values at the  $\gamma$  position are often notably more negative than those at

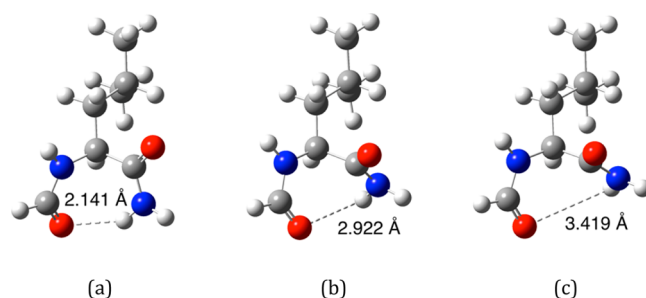


**Figure 4.** Structure of **1**: (a) fully optimized; (b) within the transition structure of  $\alpha$  abstraction by  $\text{Cl}^\bullet$ ; (c) within the transition structure of  $\alpha$  abstraction by  $\text{OH}^\bullet$ .

other positions. We find that abstraction from the  $\gamma$  carbon nicely positions the incoming  $\text{Cl}^\bullet$  or (especially)  $\text{OH}^\bullet$  radical for favorable secondary interactions with an  $\alpha$  substituent (Figure 5). In the case of  $\text{OH}^\bullet$  abstraction from **1**, the major

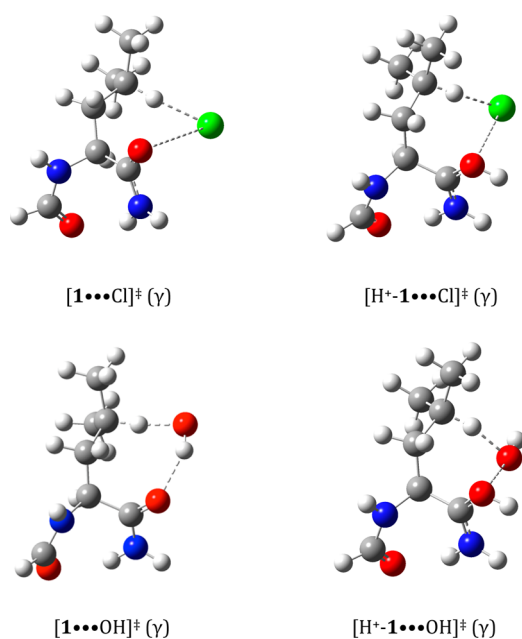


**Figure 5.** Geometry of the transition structures for abstraction from the  $\gamma$  position of **1** and  $\text{H}^+\text{-1}$  by  $\text{Cl}^\bullet$  and  $\text{OH}^\bullet$ .

secondary interaction is hydrogen bonding with an amidocarbonyl oxygen. In other cases, however, the major secondary interaction is between the amidocarbonyl oxygen and the electronegative atom (Cl or O) of the attacking radical.

We can see that, upon protonation, i.e., going from **1** to  $\text{H}^+\text{-1}$ ,  $\Delta E_{\text{int}}$  values at  $\alpha$  and  $\beta$  become less negative. This observation is consistent with a polar deactivating effect. Interestingly, for  $\text{OH}^\bullet$  abstractions from neutral **1**, the  $\alpha$   $\Delta E_{\text{int}}$  is actually the most negative among the four abstraction reactions, and this can be attributed to the hydrogen bonding between  $\text{OH}^\bullet$  and the  $\alpha$  substituents, which is in accord with previous findings.<sup>7</sup> Examination of the geometry of the corresponding transition structures at the  $\beta$ ,  $\gamma$ , and  $\delta$  positions reveals the existence of similar hydrogen-bonding interactions (see for example,  $[\text{1}\cdots\text{OH}]^\ddagger(\gamma)$  in Figure 5), but they appear to contribute to a progressively smaller extent to  $\Delta E_{\text{int}}$ .

## CONCLUDING REMARKS

Our computational study suggests that the formation of reactant complexes is unlikely to be important in determining the regioselectivity of H abstraction from the various sites in amino acid residues. Specifically, while there exist reactant complexes in enthalpic terms, entropic and solvent effects render these complexes essentially unimportant. Instead, structural factors, polar effects, and solvent effects, together with secondary interactions, can be used to rationalize the variations in the barriers. The regioselectivity of hydrogen abstraction is likely to be affected by protonation of, or hydrogen bonding to, the substrate, but reactions remote from the  $\alpha$ - and  $\beta$  positions are still favored.

## ASSOCIATED CONTENT

### Supporting Information

Optimized geometries of relevant species (Table S1) and ZPVEs, thermal corrections to enthalpies, entropies, solvation energies, and high-level single-point energies (Table S2). This material is available free of charge via the Internet at <http://pubs.acs.org>.

## AUTHOR INFORMATION

### Corresponding Author

\*E-mail: [chan\\_b@chem.usyd.edu.au](mailto:chan_b@chem.usyd.edu.au); [radom@chem.usyd.edu.au](mailto:radom@chem.usyd.edu.au).

### Present Address

<sup>||</sup>School of Chemistry, University of Tasmania, Hobart, Tasmania 7001, Australia.

### Notes

The authors declare no competing financial interest.

## ACKNOWLEDGMENTS

We gratefully acknowledge funding (to C.J.E. and L.R.) from the Australian Research Council and generous grants of computer time (to L.R.) from the NCI National Facility and Intersect Australia Ltd.

## REFERENCES

- Garrison, W. M. *Chem. Rev.* **1987**, *87*, 381–398.
- For a review, see: Easton, C. J. *Chem. Rev.* **1997**, *97*, 53–82.
- Watts, Z. I.; Easton, C. J. *J. Am. Chem. Soc.* **2009**, *131*, 11323–11325.
- For a review of experimental work, see: (a) Viehe, H. G.; Janousek, Z.; Merenyi, R.; Stella, L. *Acc. Chem. Res.* **1985**, *18*, 148–154. For theoretical studies, see for example: (b) Rauk, A.; Yu, D.; Taylor, J.; Shustov, G. V.; Block, D. A.; Armstrong, D. A. *Biochemistry* **1999**, *38*, 9089–9096. (c) Croft, A. K.; Easton, C. J.; Radom, L. *J. Am. Chem. Soc.* **2003**, *125*, 4119–4124. (d) Wood, G. P. F.; Moran, D.; Jacob, R.; Radom, L. *J. Phys. Chem. A* **2009**, *109*, 6318–6325.
- O'Reilly, R. J.; Chan, B.; Taylor, M. S.; Ivanic, S.; Bacskay, G. B.; Easton, C. J.; Radom, L. *J. Am. Chem. Soc.* **2011**, *133*, 16553–16559.
- Russell, G. A. In *Free Radicals*; Kochi, J. K., Ed.; Wiley: New York, 1973; Vol. 1, Chapter 7, pp 275–331.
- Scheiner, S.; Kar, T. *J. Am. Chem. Soc.* **2010**, *132*, 16450–16459.
- Galano, A.; Alvarez-Idaboy, J. R.; Montero, L. A.; Vivier-Bunge, A. *J. Comput. Chem.* **2001**, *22*, 1138–1153.
- Galano, A.; Alvarez-Idaboy, J. R.; Cruz-Torres, A.; Ruiz-Santoyo, M. A. *Int. J. Chem. Kinet.* **2003**, *35*, 212–221.
- Galano, A.; Alvarez-Idaboy, J. R.; Bravo-Perez, G.; Ruiz-Santoyo, M. A. *J. Mol. Struct. (THEOCHEM)* **2002**, *617*, 77–86.
- Galano, A.; Alvarez-Idaboy, J. R.; Agacino-Valdes, E.; Ruiz-Santoyo, M. E. *J. Mol. Struct. (THEOCHEM)* **2004**, *676*, 97–103.
- Galano, A.; Alvarez-Idaboy, J. R.; Cruz-Torres, A.; Ruiz-Santoyo, M. E. *J. Mol. Struct. (THEOCHEM)* **2003**, *629*, 165–174.
- (a) Chan, B.; Radom, L. *Theor. Chem. Acc.* **2011**, *130*, 251–260. (b) Chan, B.; Radom, L. *J. Phys. Chem. A* **2012**, *116*, 3745–3752.
- See, for example: (a) Hehre, W. J.; Radom, L.; Schleyer, P. v. R.; Pople, J. A. *Ab Initio Molecular Orbital Theory*; Wiley: New York, 1986. (b) Koch, W.; Holthausen, M. C. *A Chemist's Guide to Density Functional Theory*, 2nd ed.; Wiley: New York, 2001. (c) Jensen, F. *Introduction to Computational Chemistry*, 2nd ed.; Wiley: Chichester, U.K., 2007.
- Frisch, M. J.; Trucks, G. W.; Schlegel, H. B.; Scuseria, G. E.; Robb, M. A.; Cheeseman, J. R.; Scalmani, G.; Barone, V.; Mennucci, B.; Petersson, G. A.; Nakatsuji, H.; Caricato, M.; Li, X.; Hratchian, H. P.; Izmaylov, A. F.; Bloino, J.; Zheng, G.; Sonnenberg, J. L.; Hada, M.; Ehara, M.; Toyota, K.; Fukuda, R.; Hasegawa, J.; Ishida, M.; Nakajima, T.; Honda, Y.; Kitao, O.; Nakai, H.; Vreven, T.; Montgomery, J. A., Jr.; Peralta, J. E.; Ogliaro, F.; Bearpark, M.; Heyd, J. J.; Brothers, E.; Kudin,

K. N.; Staroverov, V. N.; Kobayashi, R.; Normand, J.; Raghavachari, K.; Rendell, A.; Burant, J. C.; Iyengar, S. S.; Tomasi, J.; Cossi, M.; Rega, N.; Millam, N. J.; Klene, M.; Knox, J. E.; Cross, J. B.; Bakken, V.; Adamo, C.; Jaramillo, J.; Gomperts, R. E.; Stratmann, O.; Yazyev, A. J.; Austin, R.; Cammi, C.; Pomelli, J. W.; Ochterski, R.; Martin, R. L.; Morokuma, K.; Zakrzewski, V. G.; Voth, G. A.; Salvador, P.; Dannenberg, J. J.; Dapprich, S.; Daniels, A. D.; Farkas, O.; Foresman, J. B.; Ortiz, J. V.; Cioslowski, J.; Fox, D. J. *Gaussian 09, Revision A.02*; Gaussian, Inc., Wallingford, CT, 2009.

(16) Tarnopolsky, A.; Karton, A.; Sertchook, R.; Vuzman, D.; Martin, J. M. L. *J. Phys. Chem. A* **2008**, *112*, 3–8.

(17) Curtiss, L. A.; Raghavachari, K.; Redfern, P. C.; Rassolov, V.; Pople, J. A. *J. Chem. Phys.* **1998**, *109*, 7764–7776.

(18) Merrick, J. P.; Moran, D.; Radom, L. *J. Phys. Chem. A* **2007**, *111*, 11683–11700.

(19) Hu, W.-P.; Liu, Y.-P.; Truhlar, D. G. *J. Chem. Soc., Faraday Trans.* **1994**, *90*, 1715–1725.

(20) (a) Fukui, K. *Acc. Chem. Res.* **1981**, *14*, 363–368. (b) Hratchian, H. P.; Schlegel, H. B. *J. Chem. Phys.* **2004**, *12*, 9918–9924. (c) Hratchian, H. P.; Schlegel, H. B. In *Theory and Applications of Computational Chemistry: The First 40 Years*; Dykstra, C. E., Frenking, G., Kim, K. S., Scuseria, G., Eds.; Elsevier: Amsterdam, 2005; pp 195–249.

(21) (a) Malick, D. K.; Petersson, G. A.; Montgomery, J. A., Jr. *J. Chem. Phys.* **1998**, *108*, 5704–5713. (b) Petersson, G. A. In *Computational Thermochemistry: Prediction and Estimation of Molecular Thermodynamics*; Irikura, K. K., Frurip, D. J., Eds.; American Chemical Society: Washington DC, 1998; ACS Symposium Series 677; pp 237–266.

(22) Marenich, A. V.; Cramer, C. J.; Truhlar, D. G. *J. Phys. Chem. B* **2009**, *113*, 6378–6396.

(23) The experimental standard free energy of solvation for H<sub>2</sub>O was obtained from ref 22. For OH<sup>•</sup> and HCl, the values were calculated using Henry's Law constants (29 (OH<sup>•</sup>) and 1.1 (HCl) M atm<sup>-1</sup>) obtained from: *NIST Chemistry WebBook*; Linstrom, P. J., Mallard, W. G., Eds.; National Institute of Standards and Technology; Gaithersburg, MD, 2011; NIST Standard Reference Database Number 69; <http://webbook.nist.gov> (accessed September 2012).

(24) Sandala, G. M.; Smith, D. M.; Radom, L. *Acc. Chem. Res.* **2010**, *43*, 642–651.

(25) (a) Zhong, G.; Chan, B.; Radom, L. *J. Am. Chem. Soc.* **2007**, *129*, 924–933. For other recent applications of such energy decomposition analysis, see for example: (b) Hayden, A. E.; Houk, K. N. *J. Am. Chem. Soc.* **2009**, *131*, 4084–4089. (c) Im, G.-Y. J.; Bronner, S. M.; Goetz, A. E.; Paton, R. S.; Cheong, P. H.-Y.; Houk, K. N.; Garg, N. K. *J. Am. Chem. Soc.* **2010**, *132*, 17933–17944. (d) Krenske, E. H.; Davison, E. C.; Forbes, I. T.; Warner, J. A.; Smith, A. L.; Holmes, A. B.; Houk, K. N. *J. Am. Chem. Soc.* **2012**, *134*, 2434–2441.